*J Physiol* 589.15 (2011) pp 3709–3720



The Journal of Physiology

# Alternative splicing determines mRNA translation initiation and function of human $K_{2P}10.1$ $K^+$ channels

Kathrin Staudacher, Ioana Baldea, Jana Kisselbach, Ingo Staudacher, Ann-Kathrin Rahm, Patrick A. Schweizer, Rüdiger Becker, Hugo A. Katus and Dierk Thomas

*Department of Cardiology, Medical University Hospital Heidelberg, Im Neuenheimer Feld 410, D-69120 Heidelberg, Germany*

**Non-technical summary** The resting membrane potential of excitable cells such as neurones and cardiac myocytes depends on the distribution of potassium ions across the cell membrane. Specialized membrane proteins called $K_{2P}10.1$ ion channels pass potassium ions and stabilize membranes of excitable cells at hyperpolarizing potentials below the threshold for action potential firing. Alternative mRNA translation initiation (ATI) contributes to $K_{2P}10.1$ protein diversity: Ribosomal synthesis of $K_{2P}10.1$ channel proteins harbouring different N-terminal domains initiated from two downstream mRNA start codons regulates $K_{2P}10.1$ function. We now demonstrate that splicing determines translation start sites of human $K_{2P}10.1$ mRNA via recombination of short nucleotide signalling sequences preceding the first start mRNA codon, revealing a novel biological mechanism. Our study suggests that tissue-specific $K_{2P}10.1$ ion channel mRNA splicing and translation initiation determines the resting membrane potential and contributes to electrophysiological plasticity of neuronal and cardiac cells.

**Abstract** Potassium-selective ion channels regulate cardiac and neuronal excitability by stabilizing the resting membrane potential and by modulating shape and frequency of action potentials. The delicate control of membrane voltage requires structural and functional diversity of $K^+$ channel subunits expressed in a given cell. Here we reveal a previously unrecognized biological mechanism. Tissue-specific mRNA splicing regulates alternative translation initiation (ATI) of human $K_{2P}10.1$ $K^+$ background channels via recombination of 5′ nucleotide motifs. ATI-dependent expression of full-length protein or truncated subunits initiated from two downstream start codons determines macroscopic current amplitudes and biophysical properties of $hK_{2P}10.1$ channels. The interaction between $hK_{2P}10.1$ mRNA splicing, translation and function increases $K^+$ channel complexity and is expected to contribute to electrophysiological plasticity of excitable cells.

(Received 14 April 2011; accepted after revision 6 June 2011; first published online 13 June 2011)

**Corresponding author** D. Thomas: Department of Cardiology, Medical University Hospital Heidelberg, Im Neuenheimer Feld 410, D-69120 Heidelberg, Germany.
Email: dthomas@ix.urz.uni-heidelberg.de

**Abbreviations** ATI, alternative mRNA translation initiation; $K_{2P}$, two-pore-domain potassium channel; TREK1, TWIK-related $K^+$ channel 1; TWIK, tandem of P domains in a weak inward rectifying $K^+$ channel.

K. Staudacher, I. Baldea and J. Kisselbach contributed equally to this work.



DOI: 10.1113/jphysiol.2011.210666

## Introduction

Differential regulation of mRNA translation contributes to the complexity of eukaryotic proteomes. Alternative mRNA translation initiation (ATI) creates structural and functional protein diversity. Synthesis of proteins harbouring different N-terminal domains from a single mRNA by ATI has been shown to alter subcellular localization and function of transcription and growth factors, cell cycle regulators, hormone receptors and protein kinases (Prats *et al.* 1989; Lu & Cidlowski, 2005; Rhen & Cidlowski, 2005; Cai *et al.* 2006). ATI has been implicated in cancers including Burkitt's lymphoma, T cell acute lymphoblastic leukaemia and retinoblastoma (Hann *et al.* 1988; Mellentin *et al.* 1989; Sánchez-Sánchez *et al.* 2007). Ion channels recently joined the inventory of mammalian proteins subject to ATI. The two-pore-domain $K^+$ ($K_{2P}$) channel family has 15 mammalian members (Goldstein *et al.* 2001; Thomas & Goldstein, 2009). $K_{2P}$ channels stabilize membranes of excitable cells at hyperpolarizing potentials below the threshold for action potential firing. Alternative translation initiation of $K_{2P}2.1$ (TREK1, 'tandem of P domains in a weak inward rectifying $K^+$ channel (TWIK)-related $K^+$ channel 1') channels was revealed as a novel mechanism to further increase the number of functional $K_{2P}2.1$ subunits, differentially producing two endogenous variants in regional and developmental manner in rat central nervous system (Thomas *et al.* 2008; Yang & Jan, 2008). $K_{2P}2.1$ subunit variants regulate resting membrane potential in neurones and display differences in single channel characteristics, ion selectivity and inter-subunit interactions (Thomas *et al.* 2008; Veale *et al.* 2010). Furthermore, ATI regulates expression and single channel function of $K_{2P}10.1$ (TREK2) channels that are closely related to $K_{2P}2.1$ (Honore, 2008; Simkin *et al.* 2008), indicating broader significance of this biological mechanism. Emerging evidence suggests that ATI is a regulated process (Thomas *et al.* 2008). However, molecular details about its modulation remain elusive. Here we demonstrate that differential splicing regulates ATI of human $K_{2P}10.1$ mRNA via recombination of translation initiation motifs, revealing a novel biological mechanism to create functional protein diversity.

## Methods

### Ethics approval

This study has been approved by the ethics committee of the State of Baden-Württemberg, Germany, and was carried out in accordance with the *Guide for the Care and Use of Laboratory Animals* of the US National Institutes of Health (NIH publication No. 86-23, revised 1985). The current version of the German Law on the Protection of Animals was followed, and experiments conform to the principles of UK regulations, as described in Drummond (2009).

### Molecular biology

Complementary DNAs encoding human $K_{2P}10.1$-iso1 (TREK2a) and human $K_{2P}10.1$-iso2 (TREK2c) (GenBank accession numbers EU978938 and EU978939) were amplified from a brain cDNA library (Clontech, Palo Alto, CA, USA). $K_{2P}10.1$-iso3 (TREK2b) cDNA (GenBank accession number EU978941) was amplified from a human kidney cDNA library (Clontech). Polymerase chain reaction (PCR) was carried out using nested pairs of specific oligonucleotide primers (Table 1). Complementary DNAs were inserted into the pCR2.1-TOPO vector (Invitrogen, Carlsbad, CA, USA) and subcloned into pRAT, a dual-purpose expression vector containing a CMV promoter for mammalian expression and a T7 promoter for cRNA synthesis (Bockenhauer *et al.* 2001). Tissue-specific expression of $K_{2P}10.1$ transcripts was analysed using nested PCR amplification of entire coding regions and adjacent untranslated regions using primers described above (Table 1), followed by agarose gel electrophoresis of resulting cDNAs. Human cDNA libraries (Clontech) served as templates. Mutations described in the text were made with the QuikChange Site-Directed Mutagenesis kit (Stratagene, La Jolla, CA, USA). N-terminal truncations, introduction of a C-terminal 1d4 epitope tag (ETSQVAPA; following a proline linker, RVPDGDPD) at the end of the C-terminus after removal of the stop codon, and introduction of modified translation initiation sequences was achieved using PCR. All cDNA constructs were confirmed by DNA sequencing. Complementary RNAs were transcribed after vector linearization using T7 RNA polymerase and the mMessage mMachine kit (Ambion, Austin, TX, USA). Transcripts were quantified by spectrophotometry and cRNA integrity was assessed by agarose gel electrophoresis.

### Cell culture

Human embryonic kidney (HEK 293) cells were cultured in Dulbecco's modified Eagle's medium (DMEM) supplemented with 10% fetal bovine serum, 2 mM L-glutamine, 100,000 U $l^{-1}$ penicillin, and 100 mg $l^{-1}$ streptomycin, and held at 37°C in humidified air with 5% $CO_2$. Cells were passaged regularly. Media and supplements were purchased from Invitrogen.

### Protein expression and purification with *Xenopus* oocytes and HEK 293 cells

Oocytes were isolated from *Xenopus laevis* frogs and treated with collagenase to ease removal of the follicular layer. Complementary RNA encoding study proteins

**Table 1. PCR primers used for amplification of $hK_{2P}10.1$ isoforms from human cDNA**

| Isoform | | Primer sequences (amplification product length) |
|---|---|---|
| $hK_{2P}10.1$-iso 1 | 1st PCR | Forward primer: 5′-GGAGCGTGGGGAGGGGGTAAGG-3′<br>Reverse primer: 5′-CACATAACCAGCTCCCACCCAATCAGG-3′ (2469 bp) |
| | 2nd PCR | Forward primer: 5′-CACACGGCATTCATTAAAGTGGTGGG-3′<br>Reverse primer: 5′-GGAATAGCTGCCCTTGTCTACGTGTGTGC-3′ (2266 bp) |
| $hK_{2P}10.1$-iso 2 | 1st PCR | Forward primer: 5′-TGCAAACACCCAAGCCCTCTCC-3′<br>Reverse primer: 5′-CACATAACCAGCTCCCACCCAATCAGG-3′ (2275 bp) |
| | 2nd PCR | Forward primer: 5′-TCTGGGGTTCCTCCACGAGCC-3′<br>Reverse primer: 5′-GGAATAGCTGCCCTTGTCTACGTGTGTGC-3′ (2112 bp) |
| $hK_{2P}10.1$-iso 3 | 1st PCR | Forward primer: 5′-GGAGCCTGCACTTTACTCTGAATGTTGG-3′<br>Reverse primer: 5′-CACATAACCAGCTCCCACCCAATCAGG-3′ (2183 bp) |
| | 2nd PCR | Forward primer: 5′-GTCCATGTGATCACACTGACACCTGAGAG-3′<br>Reverse primer: 5′-GGAATAGCTGCCCTTGTCTACGTGTGTGC-3′ (2024 bp) |

(15 ng oocyte$^{-1}$) was injected into 100 *Xenopus laevis* oocytes. After 2 days, oocytes were homogenized using a glass–Teflon tissue homogenizer. Protein extracts were prepared by solubilization in buffer A (100 mM NaCl, 40 mM KCl, 1 mM EDTA, 10% glycerol, 1% Chaps, 20 mM Hepes, pH 7.4) for 1 h and clarified by repeated centrifugations at 5000 *g* for 10 min, followed by a final centrifugation at 25,000 *g*. Complete Protease Inhibitor Cocktail (Roche Diagnostics, Indianapolis, IN, USA) was included in all buffer solutions used for protein preparation. The resulting supernatant was diluted with 2-mercaptoethanol-containing SDS-PAGE loading buffer and analysed by Western blotting. Representative data from three independent assays are presented.

Complementary DNA (18.75 $\mu$g cDNA/T175 flask) was transiently expressed in HEK 293 cells using FuGENE 6 transfection reagent (Roche Diagnostics) according to the manufacturer's instructions. Plates were harvested 2 days after transfection. Protein extracts were prepared by solubilization in buffer B (100 mM NaCl, 40 mM KCl, 1 mM EDTA, 10% glycerol, 1% Triton, 20 mM Hepes, pH 7.4) for 1 h and clarified by centrifugation at 50,000 x g for 30 min. The supernatant was diluted with DTT-containing SDS-PAGE loading buffer and analysed by Western blotting. Biochemical data shown were obtained from three independent assays.

## Western blot analysis

Oocyte or HEK 293 cell lysates prepared in this study were subjected to SDS-PAGE on 10% precast gels (Ready Gels, Bio-Rad, Munich, Germany) followed by wet-transfer onto PVDF membranes and Western blot analyses using anti-1d4 (1:500; overnight incubation) monoclonal (m) antibodies developed in mouse (sc-57432; Santa Cruz Biotechnology, Santa Cruz, CA, USA). Peroxidase-conjugated secondary antibodies raised in goat against mouse were obtained from Sigma-Aldrich (A9917; St Louis, MO, USA) and used at 1:10,000 dilutions (1 h incubation time). The secondary labelling of peroxidase conjugates was documented with enhanced chemiluminescence and autoradiography.

## Electrophysiology

For two-electrode voltage clamp (TEVC) recordings, 1 ng cRNA encoding study channels was injected into defolliculated *Xenopus* oocytes. Whole cell currents were measured 3 days after injection with an Oocyte Clamp amplifier (Warner Instruments, Hamden, CT, USA) using pCLAMP9 (Axon Instruments, Union City, CA, USA) software for data acquisition. Data were sampled at 2 kHz and filtered at 1 kHz. Electrodes filled with 3 M KCl. Recordings were performed under constant perfusion at room temperature, and no leak subtraction was done during the experiments. The standard extracellular solution was (in mM): 96 NaCl, 4 KCl, 1.1 $CaCl_2$, 1 $MgCl_2$, 5 Hepes (pH 7.4, adjusted with NaOH). Currents were evoked by step depolarization from −140 to +60 mV (500 ms) in 20 mV increments at 2 s intervals from the holding potential (−80 mV). Electrophysiological data presented in this work were obtained from two independent batches of oocytes expressing respective channel subunits ($n = 8$ oocytes per batch).

*A*

```
                    M1  M1                                                  M55/60
                    ↓   ↓                                                     ↓
hK2P10.1_Iso1       ----MFFLYTDFFLS-LVAVPAAAPVCQPKSATNGQPPAPAPTPTPRLSISSRATVVARM 55
hK2P10.1_Iso2       MKFPIETPRKQVNWDPKVAVPAAAPVCQPKSATNGQPPAPAPTPTPRLSISSRATVVARM 60
hK2P10.1_Iso3       MEDGFKGDRTEGCRSDSVAVPAAAPVCQPKSATNGQPPAPAPTPTPRLSISSRATVVARM 60
                        :    .:    .  ****************************************

                          M67/72
                            ↓                TM1
hK2P10.1_Iso1       EGTSQGGLQTVMKWKTVVAIFVVVVVYLVTGGLVFRALEQPFESSQKNTIALEKAEFLRD 115
hK2P10.1_Iso2       EGTSQGGLQTVMKWKTVVAIFVVVVVYLVTGGLVFRALEQPFESSQKNTIALEKAEFLRD 120
hK2P10.1_Iso3       EGTSQGGLQTVMKWKTVVAIFVVVVVYLVTGGLVFRALEQPFESSQKNTIALEKAEFLRD 120
                    ************************************************************

                                                                  P1
hK2P10.1_Iso1       HVCVSPQELETLIQHALDADNAGVSPIGNSSNNSSHWDLGSAFFFAGTVITTIGYGNIAP 175
hK2P10.1_Iso2       HVCVSPQELETLIQHALDADNAGVSPIGNSSNNSSHWDLGSAFFFAGTVITTIGYGNIAP 180
hK2P10.1_Iso3       HVCVSPQELETLIQHALDADNAGVSPIGNSSNNSSHWDLGSAFFFAGTVITTIGYGNIAP 180
                    ************************************************************

                              TM2
hK2P10.1_Iso1       STEGGKIFCILYAIFGIPLFGFLLAGIGDQLGTIFGKSIARVEKVFRKKQVSQTKIRVIS 235
hK2P10.1_Iso2       STEGGKIFCILYAIFGIPLFGFLLAGIGDQLGTIFGKSIARVEKVFRKKQVSQTKIRVIS 240
hK2P10.1_Iso3       STEGGKIFCILYAIFGIPLFGFLLAGIGDQLGTIFGKSIARVEKVFRKKQVSQTKIRVIS 240
                    ************************************************************

                          TM3                                 P2
hK2P10.1_Iso1       TILFILAGCIVFVTIPAVIFKYIEGWTALESIYFVVVTLTTVGFGDFVAGGNAGINYREW 295
hK2P10.1_Iso2       TILFILAGCIVFVTIPAVIFKYIEGWTALESIYFVVVTLTTVGFGDFVAGGNAGINYREW 300
hK2P10.1_Iso3       TILFILAGCIVFVTIPAVIFKYIEGWTALESIYFVVVTLTTVGFGDFVAGGNAGINYREW 300
                    ************************************************************

                              TM4
hK2P10.1_Iso1       YKPLVWFWILVGLAYFAAVLSMIGDWLRVLSKKTKEEVGEIKAHAAEWKANVTAEFRETR 355
hK2P10.1_Iso2       YKPLVWFWILVGLAYFAAVLSMIGDWLRVLSKKTKEEVGEIKAHAAEWKANVTAEFRETR 360
hK2P10.1_Iso3       YKPLVWFWILVGLAYFAAVLSMIGDWLRVLSKKTKEEVGEIKAHAAEWKANVTAEFRETR 360
                    ************************************************************

hK2P10.1_Iso1       RRLSVEIHDKLQRAATIRSMERRRLGLDQRAHSLDMLSPEKRSVFAALDTGRFKASSQES 415
hK2P10.1_Iso2       RRLSVEIHDKLQRAATIRSMERRRLGLDQRAHSLDMLSPEKRSVFAALDTGRFKASSQES 420
hK2P10.1_Iso3       RRLSVEIHDKLQRAATIRSMERRRLGLDQRAHSLDMLSPEKRSVFAALDTGRFKASSQES 420
                    ************************************************************

hK2P10.1_Iso1       INNRPNNLRLKGPEQLNKHGQGASEDNIINKFGSTSRLTKRKNKDLKKTLPEDVQKIYKT 475
hK2P10.1_Iso2       INNRPNNLRLKGPEQLNKHGQGASEDNIINKFGSTSRLTKRKNKDLKKTLPEDVQKIYKT 480
hK2P10.1_Iso3       INNRPNNLRLKGPEQLNKHGQGASEDNIINKFGSTSRLTKRKNKDLKKTLPEDVQKIYKT 480
                    ************************************************************

hK2P10.1_Iso1       FRNYSLDEEKKEEETEKMCNSDNSSTAMLTDCIQQHAELENGMIPTDTKDREPENNSLLE 535
hK2P10.1_Iso2       FRNYSLDEEKKEEETEKMCNSDNSSTAMLTDCIQQHAELENGMIPTDTKDREPENNSLLE 540
hK2P10.1_Iso3       FRNYSLDEEKKEEETEKMCNSDNSSTAMLTDCIQQHAELENGMIPTDTKDREPENNSLLE 540
                    ************************************************************

hK2P10.1_Iso1       DRN 538
hK2P10.1_Iso2       DRN 543
hK2P10.1_Iso3       DRN 543
                    ***
```

*B* **$hK_{2P}10.1$ translation initiation sequences (TIS)**

| | -3 | +1 | +4 |
|---|---|---|---|
| M1 ($hK_{2P}10.1$-iso1) | CUU UCU | UGG AUG | U |
| M1 ($hK_{2P}10.1$-iso2) | AAC GAA | GCA AUG | A |
| M1 ($hK_{2P}10.1$-iso3) | GGC UGG | UAU AUG | G |
| M55/60 ($hK_{2P}10.1$) | GUA GCC | AGG AUG | G |
| M67/72 ($hK_{2P}10.1$) | CAG ACC | GUC AUG | A |
| Optimal sequence | GCC GCC | A/G CC AUG | G |

### Data analysis and statistics

Origin 6 (OriginLab Corp., Northampton, MA, USA) software was used for data analysis. Data are expressed as means ± SEM. We used Student's *t* test (two-tailed tests) to compare statistical significance of the results: $P < 0.05$ was considered statistically significant. Multiple comparisons were performed using one-way ANOVA. If the hypothesis of equal means could be rejected at the 0.05 level, pairwise comparisons of groups were made and the probability values were adjusted for multiple comparisons using the Bonferroni correction.

## Results and discussion

### Tissue distribution of human $K_{2P}10.1$ splice variants

Splicing of $hK_{2P}10.1$ mRNA produces three transcript variants that differ in their N-terminal domains ($hK_{2P}10.1$-iso1, $hK_{2P}10.1$-iso2, $hK_{2P}10.1$-iso3; Fig. 1*A*) (Lesage *et al.* 2000; Gu *et al.* 2002). We found $K_{2P}10.1$ isoforms to be expressed in a tissue-specific manner (Fig. 2*A*). Expression of $hK_{2P}10.1$-iso1 was limited to the brain. In contrast, $hK_{2P}10.1$-iso2 transcripts were detected in brain, heart, pancreas, and kidney, and $hK_{2P}10.1$-iso3 was amplified from pancreas and kidney. Based on differences in spatial distribution, we hypothesized that $hK_{2P}10.1$ transcript variants might confer structural and functional differences on $hK_{2P}10.1$ protein subunits and so merited further investigation.

### $K_{2P}10.1$ $K^+$ channel subunits produced by alternative mRNA translation initiation

Translation of the most ubiquitously detected transcript, $hK_{2P}10.1$-iso2, was studied *in vitro* in *Xenopus laevis* oocytes (Fig. 2*B*). Human $K_{2P}10.1$-iso2 subunits are predicted to have 543 amino acids and a molecular mass of 60 kDa in their native form (62 kDa when produced with a C-terminal epitope tag (1d4) for ready visualization on heterologous expression in this work). Analysis of $K_{2P}10.1$-iso2 protein revealed the predicted 62 kDa protein and a smaller immunoreactive band of ∼55 kDa. This finding is consistent with ATI producing truncated $K_{2P}10.1$-iso2 subunit variants, as reported previously for this transcript variant (Simkin *et al.* 2008). Translation initiation of most eukaryotic mRNAs follows a linear scanning mechanism where the 40S ribosome is recruited to the 5′ cap structure of the mRNA followed by downstream movement until a translation initiation codon is encountered (Kozak, 1999). In most cases, the translation initiation site is the first start codon for methionine (AUG1/M1). However, if AUG1 is surrounded by a weak nucleotide context (or *Kozak* sequence) it may be used inefficiently and some ribosomes read through the site without recognition, resulting in 'leaky scanning' and translation initiation at a downstream position. A purine (preferably A) at nucleotide position −3 and guanine at +4 with respect to an AUG make the largest contribution to initiation efficiency (Kozak, 1989). Examination of $hK_{2P}10.1$-iso2 coding sequences revealed the translation initiation context at AUG1 to be relatively strong but sub-optimal compared to an optimized sequence (Fig. 1*B*) (Kozak, 1989). Thus, leaky scanning generates truncated $K_{2P}10.1$-iso2 channels via initiation at M60 (AUG2) and M72 (AUG3) codons, each bearing a −3 purine (Figs 1*B* and 2*B*). Individual elimination of downstream start codons M60 or M72 by mutation to isoleucine did not completely prevent generation of truncated $K_{2P}10.1$-iso2 subunits, indicating ribosomal use of M60 *and* M72 (Fig. 2*B*). Mutation of M60 still allows translation initiation at M72, and *vice versa*. In contrast, synthesis of truncated $K_{2P}10.1$-iso2 variants was abolished when both M60 and M72 were replaced by isoleucine residues, confirming ATI as the underlying molecular mechanism.

Next, mutant $hK_{2P}10.1$ genes were synthesized and expressed to determine properties of truncated variants in isolation (Fig. 2*C*). In these constructs, nine nucleotides of the native mRNA sequence preceded AUG2 or AUG3 to preserve the respective natural translation initiation context. The predicted topologies of $K_{2P}10.1$-iso2 constructs used in this work are summarized in Fig. 2*D*. One gene ($K_{2P}10.1$-iso2 Δ1–59) was designed to produce truncated variants starting at M60 or M72. Mutation of the downstream methionine 72 to isoleucine in this construct yields $K_{2P}10.1$-iso2 Δ1–59 M72I cDNA, selectively producing subunits starting at M60. Expression of a third gene exclusively yields channel proteins starting at M72 because codons for the first 71 residues are deleted ($K_{2P}10.1$-iso2 Δ1–71). Upon cRNA expression in *Xenopus* oocytes, protein variants were detected as expected (Fig. 2*C*). Owing to similar molecular masses (56 *versus* 54 kDa), both truncated $K_{2P}10.1$ subunits

**Figure 1. Amino acid sequence alignments and translation initiation sequences of human $K_{2P}10.1$ splice variants ($K_{2P}10.1$-iso1, $K_{2P}10.1$-iso2, $K_{2P}10.1$-iso3)**
*A*, three alternative translation initiation sites (M1, M55/60, M67/72) are indicated by arrows. Predicted transmembrane spans (TM1–TM4) and pore loops (P1 and P2) are boxed in yellow and red, respectively. *B*, nucleotide sequences surrounding the first (M1), second (M55/M60), and third (M67/M72) start site in $K_{2P}10.1$ mRNAs are compared to optimal translation initiation nucleotide context.

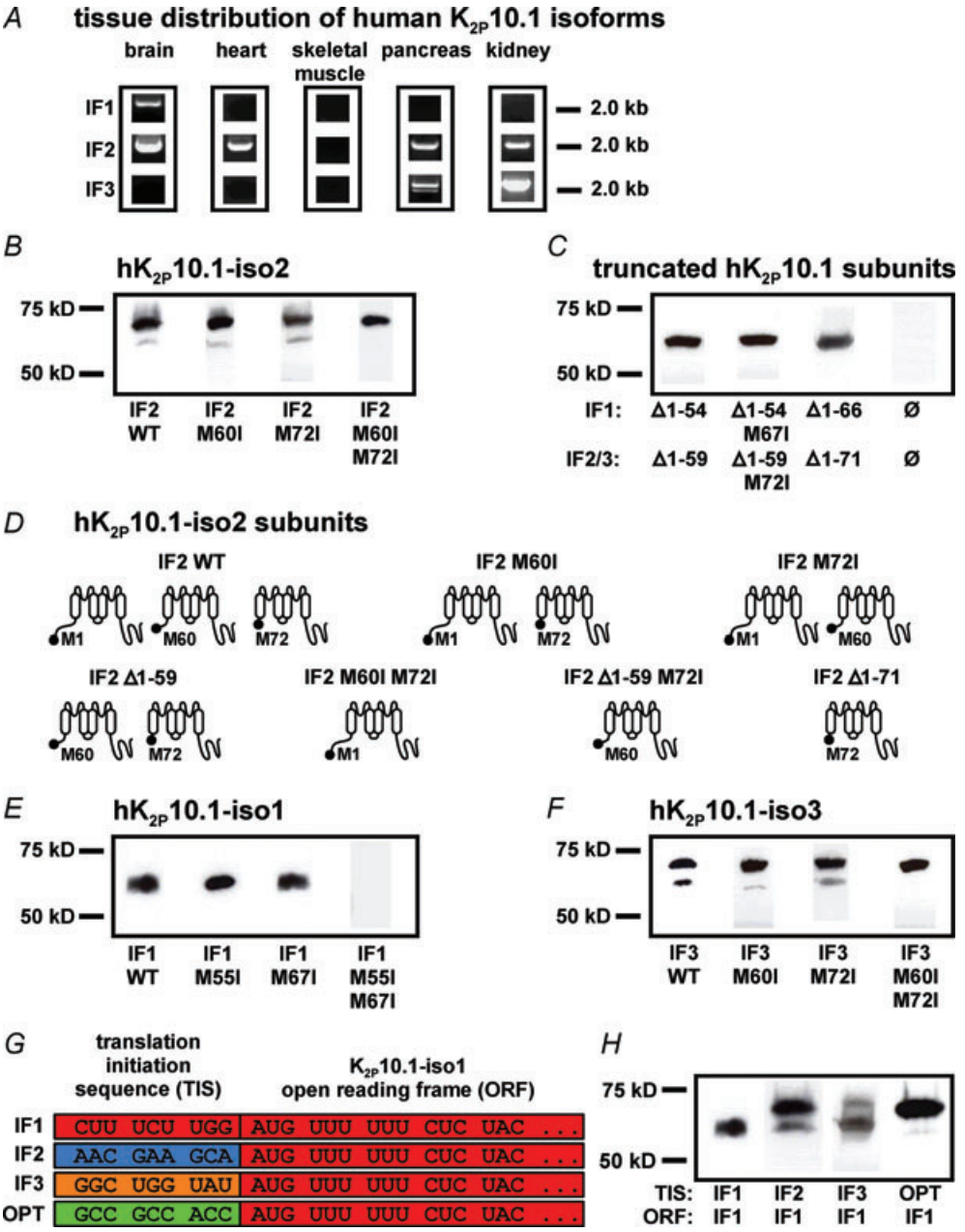


**Figure 2. Splicing of human $K_{2P}10.1$ mRNA produces structurally different $K^+$ channel subunits via alternative translation initiation (ATI)**

*A*, human tissue distribution of $K_{2P}10.1$ splice variants (IF1, $K_{2P}10.1$-iso1; IF2, $K_{2P}10.1$-iso2; IF3, $K_{2P}10.1$-iso3) assessed by PCR amplification of entire coding regions. *B*, Western blot analysis of $hK_{2P}10.1$-iso2-1d4 wild-type (IF2 WT), $hK_{2P}10.1$-iso2 M60I-1d4 (IF2 M60I), $hK_{2P}10.1$-iso2 M72I-1d4 (IF2 M72I), or $hK_{2P}10.1$-iso2 M60I M72I-1d4 (IF2 M60I M72I) subunits. *C*, protein analysis of indicated truncated $hK_{2P}10.1$–1d4 subunits (see text for details). *D*, topology of $hK_{2P}10.1$-iso2 protein variants arising from alternative mRNA translation initiation. *E* and *F*, Western blot analysis of oocytes expressing $hK_{2P}10.1$-iso1-1d4 wild-type (IF1 WT; E), $hK_{2P}10.1$-iso3-1d4 wild-type (IF3 WT; *F*), and indicated mutant cRNAs. *G*, recombination of translation initiation sequences (TIS). TIS from $hK_{2P}10.1$ isoforms 1–3 (IF1–3) and artificial optimal TIS (OPT) preceded the open reading frame (ORF) of $hK_{2P}10.1$-iso1-1d4 mRNA. *H*, translation initiation sequences differentially determine $hK_{2P}10.1$-iso1 subunit expression. Western blots of proteins produced by expression of recombinant cRNAs described in panel *G*. $K_{2P}10.1$ subunits were expressed in *Xenopus* oocytes and visualized with anti-1d4 antibody.

starting at downstream start codons M60 or M72 were indistinguishable from one other. Control oocytes did not exhibit $K_{2P}10.1$ immunoreactivity (Fig. 2*C*).

## Splicing regulates $K_{2P}10.1$ mRNA translation initiation through recombination of 5′ nucleotide sequences

$K_{2P}10.1$ transcripts 1–3 display largely similar primary structures (Fig. 1*A*) and are equally sensitive to protein kinase regulation (Gu *et al.* 2002), but exhibit significantly different translation initiation sequences at AUG1 (Fig. 1*B*). We hypothesized that splicing serves to recombine $K_{2P}10.1$ *Kozak* sequences and to determine translation initiation and protein subunit expression. The *Kozak* translation initiation context at AUG1 of $K_{2P}10.1$-iso1 is sub-optimal compared to the downstream translation context at AUG2 or AUG3 due to a purine at position −3 in the latter cases. These sequences rationalize the basis for preferential production of truncated channels as ready downstream translation initiation due to leaky ribosome scanning of $K_{2P}10.1$-iso1 mRNA. Indeed, injection of $K_{2P}10.1$-iso1 mRNA into oocytes exclusively yielded truncated subunits (Fig. 2*E*). Translation initiation occurring at both downstream codons was demonstrated by selective mutagenesis of M55 or M67, as described above for $K_{2P}10.1$-iso2. In contrast, there was no $K_{2P}10.1$ signal after elimination of both M55 and M67 (Fig. 2*E*), indicating the lack of mRNA translation initiation at AUG1 and confirming the regulatory impact of translation initiation nucleotide sequences. $K_{2P}10.1$-iso3 displayed an intermediate biochemical phenotype (Fig. 2*F*) that is readily explained by guanine at nucleotide position +4 that increases translation initiation at M1 compared to isoform 1 (Fig. 1*B*). Of note, analysis of amino acid sequences of isoforms 1–3 revealed identical primary structures of truncated $K_{2P}10.1$ proteins, starting either at AUG2 or AUG3 downstream start codons (Fig. 1*A*). Thus, splicing and alternative mRNA translation in combination produce five different $K_{2P}10.1$ protein subunits (i.e. three isoform-specific full-length channels and two truncated subunits).

The hypothesis that expression of full-length and truncated $K_{2P}10.1$ protein is determined by splicing-dependent translation initiation signals was confirmed by experimental recombination of the $K_{2P}10.1$-iso1 coding region with native *Kozak* sequences obtained from transcripts 1–3 and with an optimized initiation sequence (Fig. 2*G*). Western blot analysis revealed differences in relative $K_{2P}10.1$ subunit expression that were determined solely by the translation initiation sequence (TIS) in the presence of identical open reading frames (ORFs) (Fig. 2*H*). $K_{2P}10.1$-iso1 wild-type cRNA did not produce full-length protein at all owing to its weak native TIS. In contrast, use of isoform 2 TIS induced translation initiation at AUG1, resulting in significant amount of full-length protein (Fig. 2*H*). The $K_{2P}10.1$-iso3 translation initiation signal triggered ribosomal translation at AUG1 as well, albeit with reduced efficacy compared to isoform 2 TIS. This observation may be explained by analysis of individual TIS strength (Fig. 1*B*). Recombination of *Kozak* sequences (Fig. 2*H*) did not fully reconstitute subunit ratios observed with wild-type $K_{2P}10.1$-iso2 (Fig. 2*B*) or $K_{2P}10.1$-iso3 (Fig. 2*F*). This is attributed to the native $K_{2P}10.1$-iso1 translation initiation nucleotide at position +4: recombination of this nucleotide was prevented as it is located within the open reading frame.

## Alternative $hK_{2P}10.1$ translation initiation in mammalian cells

Biochemical key observations from cRNA expression studies in oocytes were extended to cDNA expression in mammalian cells. In human embryonic kidney (HEK 293) cells, expression of human $K_{2P}10.1$-iso1, $K_{2P}10.1$-iso2 and $K_{2P}10.1$-iso3 cDNA, or recombination of translation initiation sequences preceding $K_{2P}10.1$-iso1 coding region revealed protein patterns that resembled our previous findings in oocytes (Fig. 3*A* and *B*). HEK 293 cells transfected with empty vector (Fig. 3*A*) served as controls and did not show $K_{2P}10.1$ signals. Biochemical evidence for

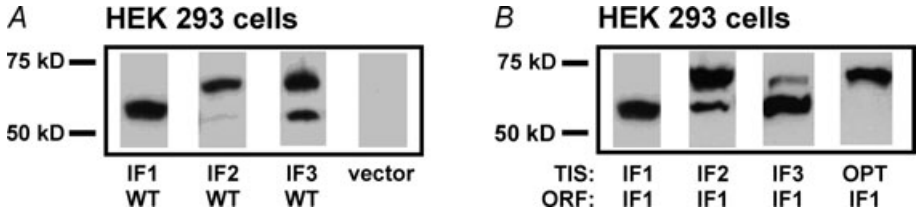


**Figure 3. $K_{2P}10.1$ isoforms in human cells**
*A*, Western blot analysis of HEK 293 cells expressing $hK_{2P}10.1$-iso1-1d4, $hK_{2P}10.1$-iso2-1d4, $hK_{2P}10.1$-iso3-1d4, or empty vector, respectively. $K_{2P}10.1$ subunits were visualized with anti-1d4 antibody. *B*, alternative mRNA translation initiation resulting from expression of $hK_{2P}10.1$-iso1-1d4 harbouring the native translation initiation sequence (TIS) is compared with synthetic constructs carrying either initiation motifs obtained from $hK_{2P}10.1$-iso2 or $hK_{2P}10.1$-iso3, or an optimized initiation motif (OPT). ORF, open reading frame.

alternative translation initiation of endogenous $K_{2P}10.1$ is provided by Kang *et al.* (2007). Using a C terminal anti-$K_{2P}10.1$ antibody, the authors detected two immunoreactive protein bands of expected molecular weight in human keratinocyte-derived HaCaT cells.

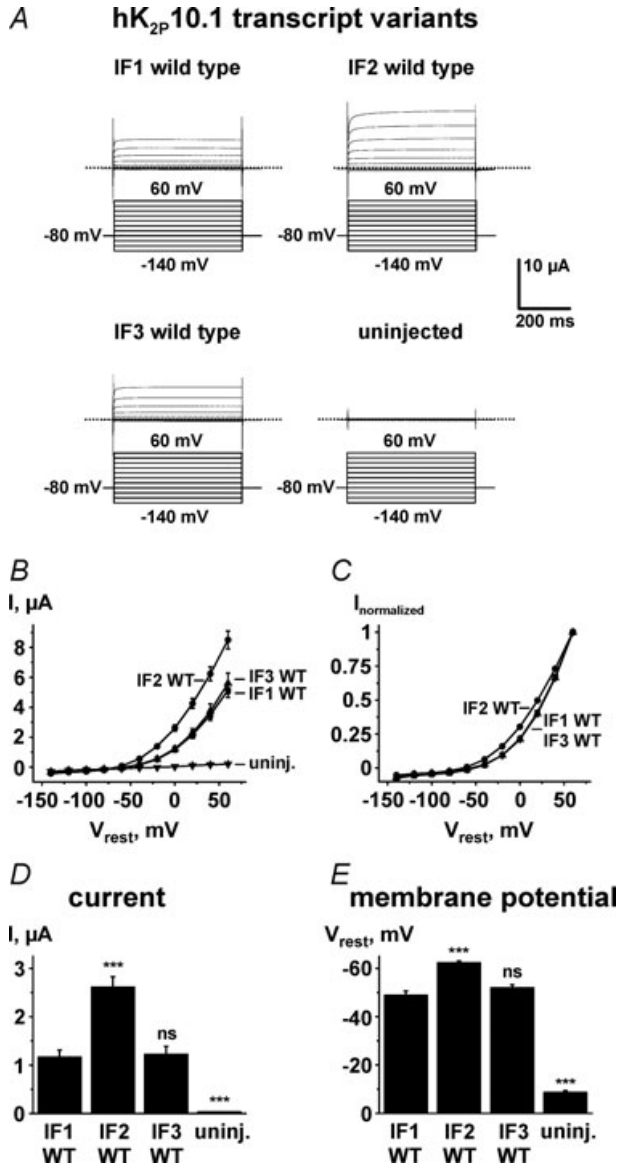


**Figure 4. Functional effects of alternative $hK_{2P}10.1$ mRNA splicing and translation initiation**
Human wild-type $K_{2P}10.1$-iso1, $hK_{2P}10.1$-iso2, or $hK_{2P}10.1$-iso3 channels studied in *Xenopus* oocytes by two-electrode voltage clamp using indicated voltage protocols. *A*, representative current families. *B* and *C*, $K_{2P}10.1$ voltage dependence of activation. Step current amplitudes as function of test potentials recorded under isochronal conditions are shown (*B*, original current amplitudes; *C*, values normalized to maximum currents; $n = 16$). *D*, mean outward currents at steady-state evoked by steps to 0 mV ($n = 16$). *E*, mean resting membrane potentials ($V_{rest}$) are displayed for groups of 16 cells. Dotted lines indicate zero current levels. Error bars represent SEM; WT, wild-type. ***$P < 0.001$; ns, not significant *versus* $K_{2P}10.1$-iso1 wild-type subunits.

## ATI of $hK_{2P}10.1$ mRNA determines ion channel function

Functional relevance of $hK_{2P}10.1$ ATI is suggested by organ-specific mRNA splicing that recombines translation initiation sequences to determine individual $K^+$ channel subunit expression profiles. To assess the effect of splicing and ATI on $K_{2P}10.1$ function, the channels were studied in oocytes using two-electrode voltage clamp electrophysiology (Fig. 4). Expression of $K_{2P}10.1$ wild-type cRNAs displayed $K^+$ currents with electrophysiological characteristics typical for a potassium-selective background leak conductance (Fig. 4*A*–*C*). Compared to cells expressing $K_{2P}10.1$-iso1 wild-type transcript ($I_{0mV}$, $1.17 \pm 0.15\,\mu$A; $n = 16$), $K_{2P}10.1$-iso2 yielded potassium currents of greater magnitude ($I_{0mV}$, $2.61 \pm 0.22\,\mu$A; $n = 16$; $P < 0.001$) whereas $K_{2P}10.1$-iso3 had currents that remained indistinguishable from $K_{2P}10.1$-iso1 ($I_{0mV}$, $1.22 \pm 0.17\,\mu$A; $n = 16$; $P > 0.05$) (Fig. 4*D*). Human $K_{2P}10.1$ current–voltage (*I–V*) relationships were investigated under isochronal recording conditions (Fig. 4*B* and *C*), revealing minor aberrations in the $K_{2P}10.1$-iso2 *I–V* shape that could be explained by increased macroscopic currents as $K_{2P}$ rectification depends on current magnitude. Isoform-dependent effects on $K_{2P}10.1$ currents were accompanied by changes in resting membrane potential ($V_{rest}$) (Fig. 4*E*). Oocytes expressing $K_{2P}10.1$-iso1 and $K_{2P}10.1$-iso3 had resting potentials of $-48.8 \pm 1.8$ mV ($n = 16$) and $-51.9 \pm 1.3$ mV ($n = 16$), respectively. In contrast, $K_{2P}10.1$-iso2 channel expression hyperpolarized the membrane to $-62.4 \pm 0.7$ mV ($n = 16$; $P < 0.001$). We hypothesize that reduced $K_{2P}10.1$-iso1 and $K_{2P}10.1$-iso3 current and moderate $V_{rest}$ depolarization *in vivo* will initiate more ready action potential firing of excitable cells, while increased $I_{K2P10.1\text{-}iso2}$ and associated $V_{rest}$ hyperpolarization is expected to cause hypoexcitability.

## Electrophysiological properties of single $hK_{2P}10.1$ subunits

Translation of $K_{2P}10.1$ mRNA produces up to three different subunits *per* transcript, determined by translation initiation at the respective first (AUG1), second (AUG2), or third start codon (AUG3). Macroscopic electrophysiological characteristics of subunits in isolation were analysed by expressing cRNA constructs that selectively encode single subunits of $hK_{2P}10.1$ splice isoforms in *Xenopus* oocytes, as described (Fig. 2). Expression of full-length $hK_{2P}10.1$-iso1 subunits yielded reduced outward currents compared to channels formed by truncated protein resulting from ATI at AUG2 (Fig. 5). This finding is readily explained by weak sequence context and very low translation initiation at AUG1

in this isoform, resulting in virtually no full-length $hK_{2P}10.1$-iso1 protein after removal of AUG2 and AUG3 ($hK_{2P}10.1$-iso1 M55I M67I; Fig. 2*E*). Compared to intermediate length $hK_{2P}10.1$-iso1 Δ1–54 M67I subunits, $hK_{2P}10.1$-iso1 Δ1–66 channels formed by truncated protein starting AUG3 displayed low current amplitudes (Fig. 5*A*), indicating reduced translation efficacy that may be attributed to weaker *Kozak* sequences preceding AUG3 compared to AUG2 in transcript variant 1 (Fig. 1*B*). Similar observations were made upon comparison of truncated $hK_{2P}10.1$ subunits when isoforms 2 and 3 were analysed (Fig. 5*B* and *C*). In contrast to transcript variant 1, functional expression of full-length $hK_{2P}10.1$-iso2 or $hK_{2P}10.1$-iso3 yielded larger current amplitudes (Fig. 5*B* and *C*), corresponding to stronger *Kozak* sequence context and higher translation efficacy at AUG1 (Figs 1*B*, 2*B* and *F*). In all subunits investigated here, reduced macroscopic $hK_{2P}10.1$ currents were associated with resting membrane potential depolarization (Fig. 5*A*–*C*), which is in line with the physiological role of $K_{2P}$ background channels.

## Translational regulation of $K_{2P}10.1$ $K^+$ channel function

Macroscopic $hK_{2P}10.1$ currents are determined by differential subunit expression and biophysical channel properties. Here, $K_{2P}10.1$-iso2 current amplitudes are mediated by high relative expression of full-length subunits and by moderate additional translation initiation starting at AUG2 and AUG3 (Fig. 2*B*). Full-length $K_{2P}10.1$-iso2 and truncated $K_{2P}10.1$-iso2 Δ1–59 M72I subunits (Fig. 5*B*) primarily define $K_{2P}10.1$-iso2 wild-type currents (Fig. 6), as $K_{2P}10.1$-iso2 Δ1–71 carries little current (Fig. 5*B*). Reduced $K_{2P}10.1$-iso1 currents are readily explained by lack of AUG1 translation initiation (Fig. 2*E*). Therefore, $K_{2P}10.1$-iso1 current levels are carried virtually exclusively by $K_{2P}10.1$-iso1 Δ1–54 M67I subunits that produce significant currents when studied in isolation (Fig. 5*A*). $K_{2P}10.1$-iso1 Δ1–66 proteins mediate little current, and their relative contribution is minimal (Figs 5*A* and 6). Finally, $K_{2P}10.1$-iso3 currents exhibit subunit expression similar to transcript variant 2 (Fig. 6),

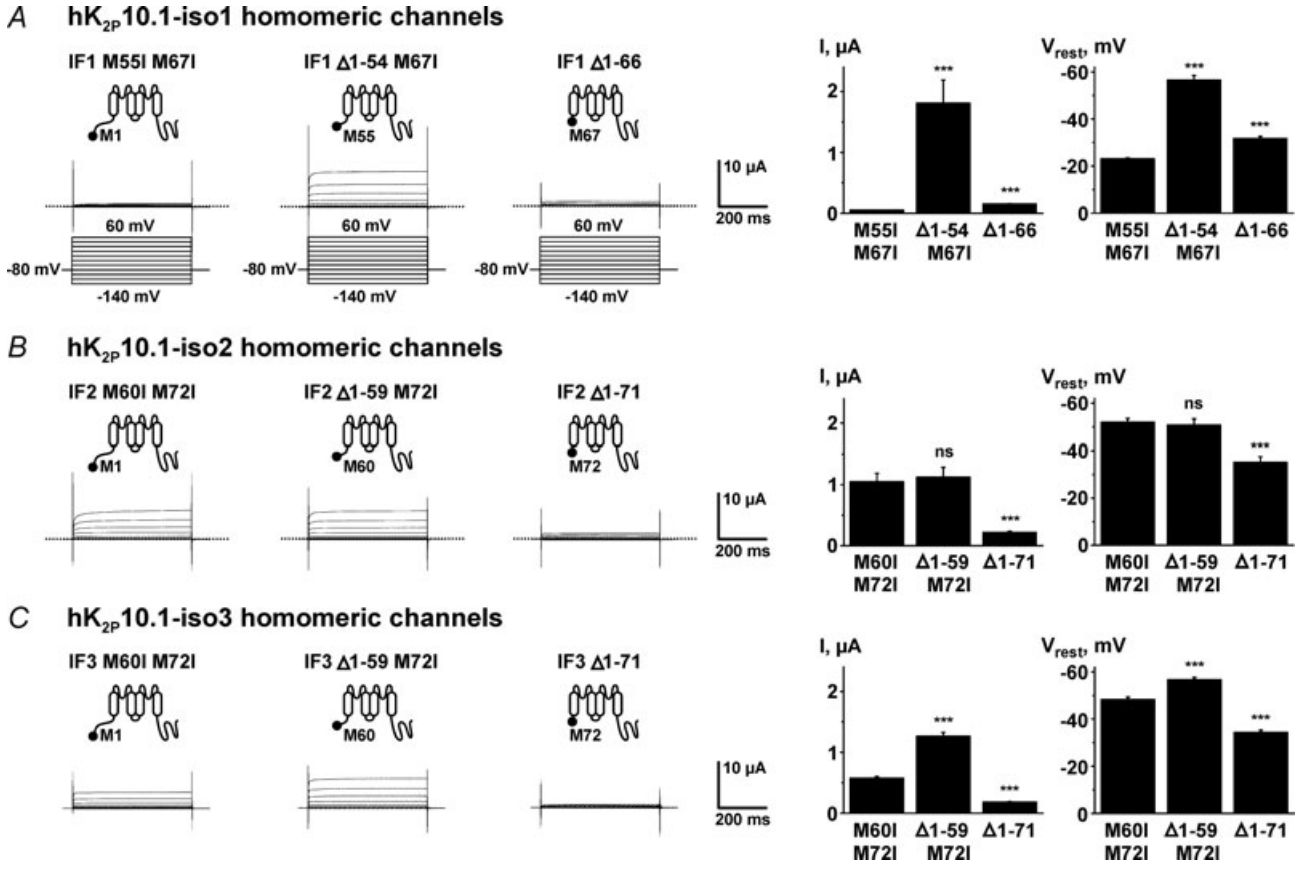


**Figure 5. Biophysical characteristics of $hK_{2P}10.1$ subunits studied in isolation**
Homomeric $hK_{2P}10.1$-iso1 (*A*), $hK_{2P}10.1$-iso2 (*B*), or $hK_{2P}10.1$-iso3 (*C*) channels formed by indicated subunits were studied in *Xenopus* oocytes by two-electrode voltage clamp. Voltage protocols are depicted in panel *A*. Representative current families, mean outward currents at steady-state evoked by steps to 0 mV, and mean resting membrane potentials ($V_{rest}$) are displayed for groups of 16 cells. Error bars represent SEM; dotted lines indicate zero current levels. ***$P < 0.001$; ns, not significant *versus* respective full-length subunits.

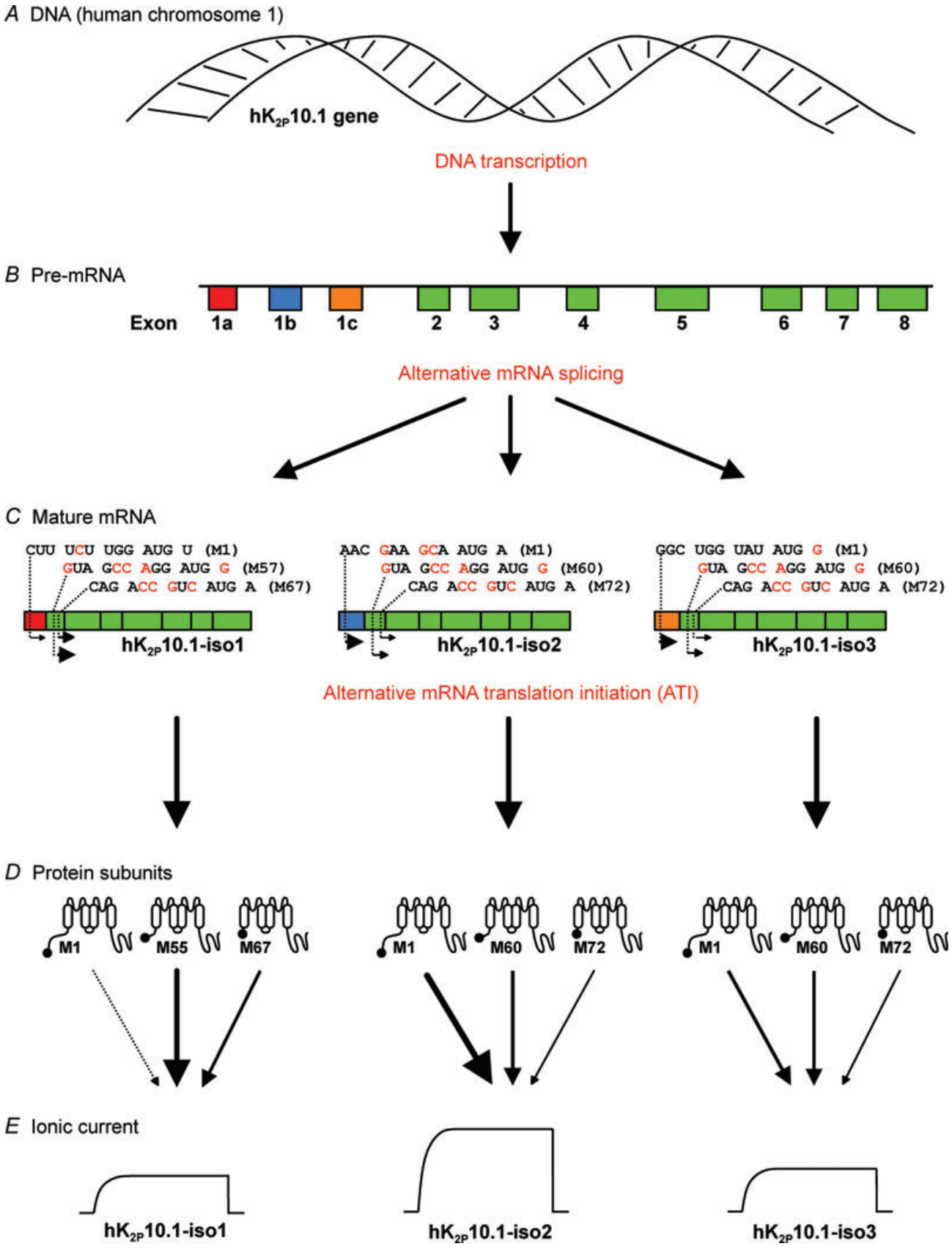

albeit with reduced relative translation initiation at AUG1 (Fig. 2*F*) that accounts for lower overall current levels compared to $K_{2P}10.1$-iso2 (Fig. 4*D*).

In conclusion, alternative mRNA translation initiation controls macroscopic currents, biophysical characteristics, and single channel properties of $hK_{2P}10.1$ $K^+$ leak channels. Our data reveal recombination of translation initiation signals through $K_{2P}10.1$ mRNA splicing that exhibits distinct spatial distribution in humans. This previously unrecognized biological interaction between mRNA splicing and translation increases ion channel diversity and is expected to contribute to electrophysiological plasticity *in vivo*.

## References


Bockenhauer D, Zilberberg N & Goldstein SA (2001). KCNK2: reversible conversion of a hippocampal potassium leak into a voltage-dependent channel. *Nat Neurosci* **4**, 486–491.

Cai J, Huang Y, Li F & Li Y (2006). Alteration of protein subcellular location and domain formation by alternative translational initiation. *Proteins* **62**, 793–799.

Drummond GB (2009) Reporting ethical matters in *The Journal of Physiology*: standards and advice. *J Physiol* **587**, 713–719.

Goldstein SA, Bockenhauer D, O'Kelly I & Zilberberg N (2001). Potassium leak channels and the KCNK family of two-P-domain subunits. *Nat Rev Neurosci* **2**, 175–184.

Gu W, Schlichthörl G, Hirsch JR, Engels H, Karschin C, Karschin A, Derst C, Steinlein OK & Daut J (2002). Expression pattern and functional characteristics of two novel splice variants of the two-pore-domain potassium channel TREK-2. *J Physiol* **539**, 657–668.

Hann SR, King MW, Bentley DL, Anderson CW & Eisenman RN (1988). A non-AUG translational initiation in c-myc exon 1 generates an N-terminally distinct protein whose synthesis is disrupted in Burkitt's lymphomas. *Cell* **52**, 185–195.

Honoré E (2008). Alternative translation initiation further increases the molecular and functional diversity of ion channels. *J Physiol* **586**, 5605–5606.

Kang D, Kim SH, Hwang EM, Kwon OS, Yang HY, Kim ES, Choi TH, Park JY, Hong SG & Han J (2007). Expression of thermosensitive two-pore domain $K^+$ channels in human keratinocytes cell line HaCaT cells. *Exp Dermatol* **16**, 1016–1022.

Kozak M (1989). The scanning model for translation: an update. *J Cell Biol* **108**, 229–241.

Kozak M (1999). Initiation of translation in prokaryotes and eukaryotes. *Gene* **234**, 187–208.

Lesage F, Terrenoire C, Romey G & Lazdunski M (2000). Human TREK2, a 2P domain mechano-sensitive $K^+$ channel with multiple regulations by polyunsaturated fatty acids, lysophospholipids, and $G_s$, $G_i$, and $G_q$ protein-coupled receptors. *J Biol Chem* **275**, 28398–28405.

Lu NZ & Cidlowski JA (2005). Translational regulatory mechanisms generate N-terminal glucocorticoid receptor isoforms with unique transcriptional target genes. *Mol Cell* **18**, 331–342.

Mellentin JD, Smith SD & Cleary ML (1989). lyl-1, a novel gene altered by chromosomal translocation in T cell leukemia, codes for a protein with a helix-loop-helix DNA binding motif. *Cell* **58**, 77–83.

Prats H, Kaghad M, Prats AC, Klagsbrun M, Lélias JM, Liauzun P, Chalon P, Tauber JP, Amalric F, Smith JA & Caput D (1989). High molecular mass forms of basic fibroblast growth factor are initiated by alternative CUG codons. *Proc Natl Acad Sci U S A* **86**, 1836–1840.

Rhen T & Cidlowski JA (2005). Antiinflammatory action of glucocorticoids – new mechanisms for old drugs. *N Engl J Med* **353**, 1711–1123.

Sánchez-Sánchez F, Ramírez-Castillejo C, Weekes DB, Beneyto M, Prieto F, Nájera C & Mittnacht S (2007). Attenuation of disease phenotype through alternative translation initiation in low-penetrance retinoblastoma. *Hum Mutat* **28**, 159–167.

Simkin D, Cavanaugh EJ & Kim D (2008). Control of the single channel conductance of K2P10.1 (TREK-2) by the amino-terminus: role of alternative translation initiation. *J Physiol* **586**, 5651–5663.

Thomas D & Goldstein SAN (2009). Two-P-domain ($K_{2P}$) potassium channels: leak conductance regulators of excitability. In *Encyclopedia of Neuroscience*, ed. Squire LR, pp. 1207–1220. Academic Press: Oxford, UK.

Thomas D, Plant LD, Wilkens CM, McCrossan ZA & Goldstein SA (2008). Alternative translation initiation in rat brain yields K2P2.1 potassium channels permeable to sodium. *Neuron* **58**, 859–870.

Veale EL, Rees KA, Mathie A & Trapp S (2010). Dominant negative effects of a non-conducting TREK1 splice variant expressed in brain. *J Biol Chem* **285**, 29295–29304.

Yang SB & Jan LY (2008). Thrilling moment of an inhibitory channel. *Neuron* **58**, 823–824.


## Author contributions

K.S., I.S. and A.K.R. expressed $hK_{2P}10$ cRNAs in *Xenopus* ooctyes, and collected and analysed electrophysiological data;

**Figure 6. Alternative splicing controls mRNA translation initiation and function of human $K_{2P}10.1$ channels**
Transcription of $K_{2P}10.1$ DNA (*A*) generates pre-mRNA (*B*) which is subjected to alternative splicing, yielding three different mature mRNA transcripts (*C*) with distinct translation initiation sequences surrounding the first start codon. Alternative ribosomal use of three translation initiation sites on each mature $K_{2P}10.1$ mRNA results in differential expression of protein subunit variants that differ in their N termini (*D*). Arrows indicate functional subunit expression and relative contribution to macroscopic currents. *E*, individual subunit ratios determine $K_{2P}10.1$ $K^+$ current amplitudes.

K.S., I.B. and J.K. performed $hK_{2P}10$ protein expression, purification and immunoblots in *Xenopus* oocytes and HEK 293 cells; J.K. amplified $hK_{2P}10$ from tissue-specific cDNA; P.A.S. helped with cloning and optimization of protein expression and purification; K.S., I.B., J.K., P.A.S. and D.T. conceived the experiments; I.B., J.K. and D.T. prepared the figures; K.S., I.B., J.K. and D.T. wrote the manuscript; P.A.S., R.B. and H.A.K. edited the manuscript for important intellectual content; and D.T. supervised the work. All of the authors approved the final version of the manuscript.

## Acknowledgements

We thank E. Ficker and B. Thomas for helpful suggestions and critical readings of the manuscript, and S. Bauer, R. Bloehs, J. Gütermann and B. Menrath for technical assistance. This work was supported by grants from the German Research Foundation (FRONTIERS programme to D.T.), the ADUMED-Foundation (to D.T.), the German Heart Foundation/German Foundation of Heart Research (to D.T.), and the Max Planck Society (TANDEM program to P.A.S.).